Influence of tacticity of poly(methyl methacrylate) on the compatibility with poly(vinylidene fluoride)

E. Roerdink and G. Challa
Department of Polymer Chemistry, State University of Groningen, Groningen, The Netherlands
(Received 6 September 1977)

A calorimetric study was carried out on blends of poly(vinylidene fluoride) (PVF_2), and isotactic, atactic and syndiotactic poly(methyl methacrylate) (i-, a-, and s-PMMA). The occurrence of single glass transitions over a broad composition range, as well as the lowering of the crystallization and melting temperatures of PVF_2, indicated a complete compatibility of PVF_2 with i-, a-, and s-PMMA. The measured T_g values followed Gordon–Taylor's rule with k values of 2.38, 1.72, and 1.39 for the systems of PVF_2 with i-, a-, and s-PMMA, respectively, leading to new values of the jump Δe of the thermal specific expansivity at the glass transition: 1.9×10^{-4} cm^3/g K for PVF_2 and 2.6×10^{-4} for s-PMMA. From the melting point depressions of PVF_2 crystals, it appeared that the interaction of PVF_2 segments with i-PMMA segments is stronger than with s-PMMA segments. A thermodynamic analysis of the melting point depressions after crystallization of PVF_2 at a constant relative undercooling of 0.07 resulted in values of the binary interaction parameter of about −0.1 and 0 for PVF_2 with i- and s-PMMA, respectively.

INTRODUCTION

The compatibility of poly(vinylidene fluoride) (PVF_2) with commercial poly(methyl methacrylate) (PMMA) has been reported by several authors[1-3].

The occurrence of a single glass transition in the blends and the negativity of the interaction parameter were considered as proof of compatibility. We found it interesting both from a practical and a theoretical point of view to study the mixing behaviour of PVF_2 with PMMAs of different tacticities.

The strongly different glass transition temperatures of PVF_2 (−45°C) on the one hand and i- or s-PMMA (50° and 130°C, respectively) on the other hand, enabled us to study the blends over a broad temperature range. Moreover, the PVF_2/i-PMMA system offers a unique possibility of studying the crystallization behaviour of a mixture of two compatible and crystallizable polymers.

The influence of tacticity on the compatibility of two polymers has already been qualitatively studied for the PMMA/PVC system[4]. With a crystallizable component like PVF_2, the occurrence of melting point depression offers the possibility of studying the influence of tacticity in a semi-quantitative way also.

EXPERIMENTAL

The polymers i- and s-PMMA were prepared according to known procedures[5,6], a-PMMA was an ICI product (Diakon MO/900), and the PVF_2 resin (KF polymer) was obtained in granular form from the Kureha Chemical Industry Co. Ltd. The tacticities of the PMMA samples were measured on 5% solutions in *o*-dichlorobenzene at 160°C by 60 MHz n.m.r. spectroscopy with a Varian A60 instrument[7]. $[\eta]$ of the PMMA samples were determined in chloroform at 25°C. For the calculation of $\bar{M}_v$ we used the relationship[8]: $[\eta] = 4.8 \times 10^{-5} \bar{M}_v^{0.8}$. $[\eta]$ of our PVF_2 was determined in *N,N*-dimethylformamide at 25°C and amounted to 1.03 dl/g.

Blends of PMMA and PVF_2 were prepared by coprecipitation from a common 3 wt% DMF solution in a hundredfold volume of water. After washing with water, the samples were dried for 24 h at 50°C under reduced pressure, and heated for about 30 min at 200°C to remove the solution history. The melting and crystallization temperatures, T_m and T_c, were measured with a Perkin–Elmer differential scanning calorimeter (DSC I B) at a heating rate of 8°C/min. The maximum of a melting endotherm was taken as melting temperature. A Perkin–Elmer DSC II was used to measure the glass transition temperatures T_g, at a heating rate of 10°C/min. The inflection point of the c_p curve was taken as T_g[9]. Reproducible results were obtained after a first scan.

RESULTS

T_g *measurements of quenched samples*

Figure 1 shows some characteristic thermograms of PVF_2/i-PMMA blends after quenching from the melt in liquid nitrogen.

Table 1 Data for PMMA polymers used

	$[\eta]$ (dl/g)	$\bar{M}_v \times 10^{-3}$	Triads I	H	S
i-PMMA	0.77	180	92	6	2
a-PMMA	0.40	80	5	32	63
s-PMMA	1.86	540	1	9	90

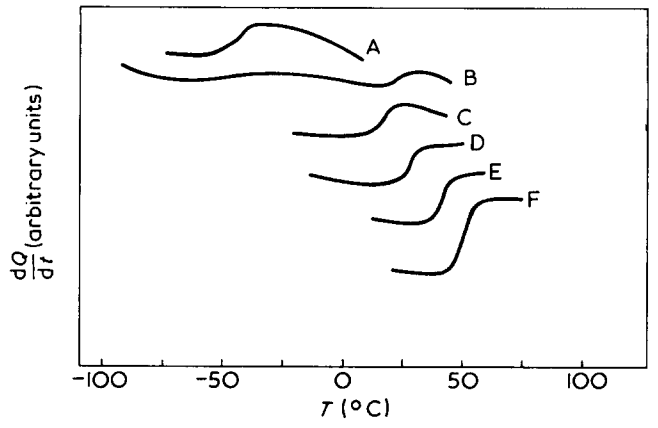

Figure 1 Thermograms of PVF_2/i-PMMA blends recorded by d.s.c. at a heating rate of 10°C/min, after quenching from the melt in liquid nitrogen. Ratio PVF_2: i-PMMA: A, 100:0; B, 80:20; C, 60:40; D, 40:60; E, 20:80; F, 0:100

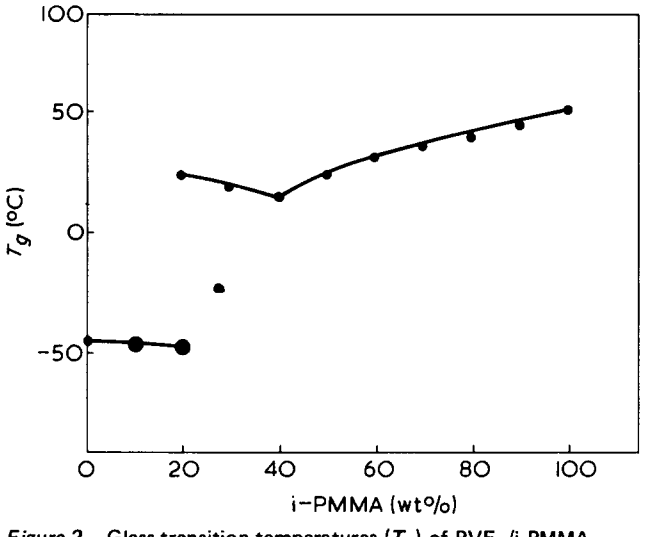

Figure 2 Glass transition temperatures (T_g) of PVF_2/i-PMMA blends after quenching from the melt in liquid nitrogen

The glass transition temperatures were derived from such thermograms and are represented in *Figures 2, 3* and *4* as a function of the weight percentage of i-, a-, and s-PMMA, respectively. Up to about 65 wt% of PVF_2 a single T_g was found which decreased smoothly with composition. However, at still higher contents T_g did not decrease further and was accompanied in some of the blends by a new broad transition at about –45°C. T_g of pure PVF_2 was also found at –45°C, and T_g of pure i-, a-, and s-PMMA at 51°, 115° and 130°C, respectively, in good agreement with values from the literature[4].

Repeated crystallization and melting

Samples were cooled from the melt with a constant cooling rate in the d.s.c. apparatus and after crystallization heated again with the same rate till melting was completed. This procedure could be repeated and gave fully reproducible crystallization and melting temperatures of the PVF_2 component *(Figure 5)*. All three types of blends show a depression of both the melting temperature and the crystallization temperature. At a cooling rate of 8°C/min PVF_2 crystallizes from blends containing up to 60 wt% i-PMMA, 50 wt% a-PMMA, and 40 wt% s-PMMA.

Isothermal crystallization

Samples of the three types of blends were crystallized at constant temperatures between 95° and 165°C in the d.s.c. apparatus. For a crystallization temperature of 155°C, the corresponding melting point curves are shown in *Figure 6*. From this Figure it is clear that the largest melting point depression is found in the blends with i-PMMA, in agreement with the T_m curves in *Figure 5* for the repeated scanning experiments. Although the melting point depressions are dependent on crystallization conditions, the largest melting point depressions of PVF_2 are always found in the blends with i-PMMA.

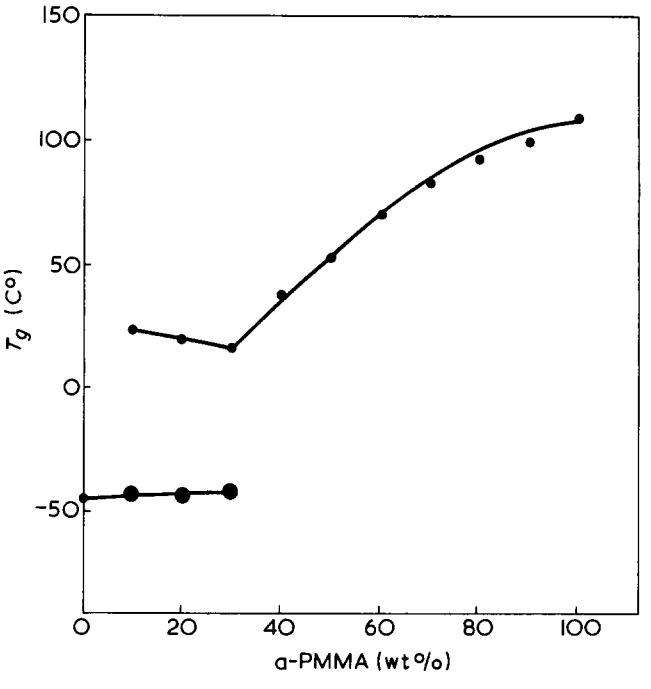

Figure 3 Glass transition temperatures (T_g) of PVF_2/a-PMMA blends after quenching from the melt in liquid nitrogen

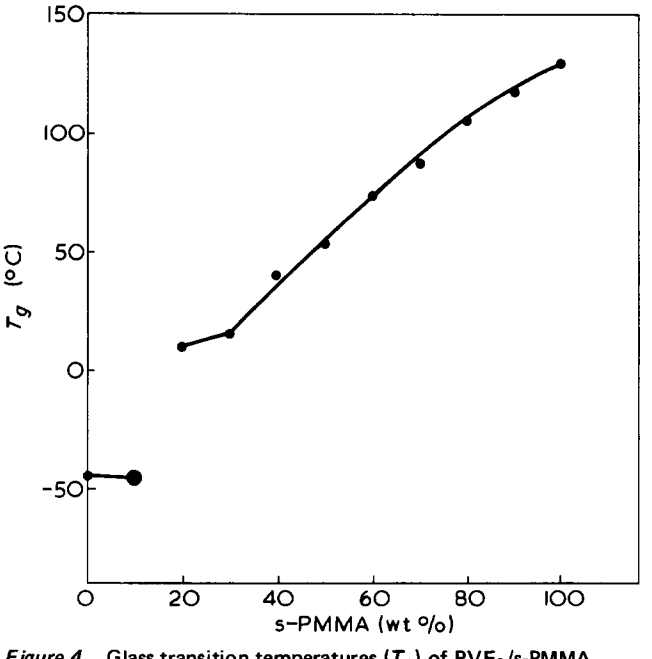

Figure 4 Glass transition temperatures (T_g) of PVF_2/s-PMMA blends after quenching from the melt in liquid nitrogen

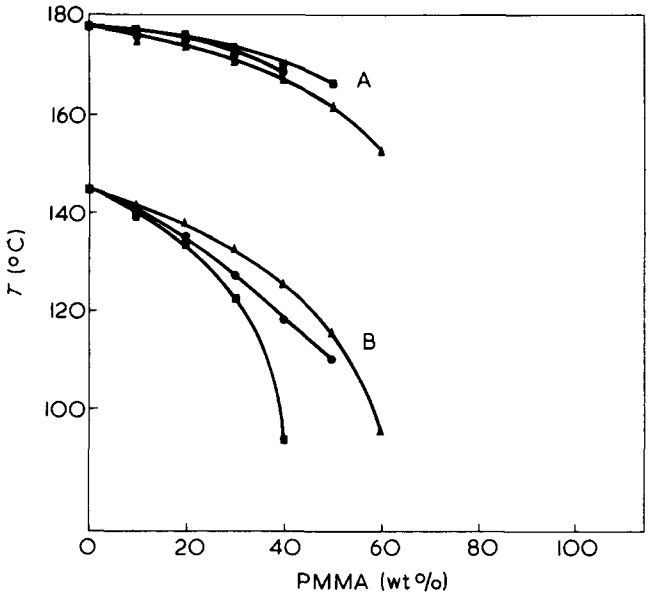

Figure 5 Crystallization and melting temperatures, T_c and T_m, of PVF_2 in PVF_2/PMMA blends measured during repeated cooling and heating in d.s.c. at 8°C/min. A, T_m; B, T_c. ▲, PVF_2/i-PMMA; ●, PVF_2/a-PMMA; ■, PVF_2/s-PMMA

DISCUSSION

Glass transitions of the blends

After quenching from the melt blends of PVF_2 with i-, a-, and s-PMMA showed only a single T_g for PVF_2 contents up to about 65 wt% (*Figures 2, 3* and *4*). So, PVF_2 proves to be compatible with each of the three kinds of PMMA in the melt phases of these blends.

Blends containing more than about 65 wt% of PVF_2 partly crystallized during quenching and could not be obtained in a completely amorphous state.

This stronger crystallization tendency of our blends compared with those of Nishi and Wang[3], might be caused by a higher content of head-to-tail units in our PVF_2. So, during scanning of a quenched blend with 30 wt% a-PMMA we found successively a broad glass transition at −45°C, a small glass transition at 15°C, only a small crystallization exotherm at 50°C, and a normal melting endotherm at 175°C. From such thermograms we concluded that a part of PVF_2 in these quenched blends was already crystalline before the scanning started. On the other hand, a quenched blend with 50 wt% a-PMMA produced a crystallization exotherm at 140°C with about the same area as that of the subsequent melting endotherm, indicating that PVF_2 in this case was completely amorphous after quenching.

The occurrence of the two glass transitions in quenched PVF_2-rich blends can now easily be explained. Part of PVF_2 is already crystalline before scanning. At higher PVF_2 contents this crystallization during quenching may proceed to a larger extent, so that the remaining amorphous phase becomes richer in PMMA, leading to a higher T_g instead of a lower one. The broad transition at about −45°C can then be attributed to cilia at the PVF_2 crystal surfaces, whereas the much sharper transition in pure PVF_2 at −45°C is caused by the totally amorphous part of PVF_2: both cilia and rejected molecules[10]. The melt viscosity of a polymer decreases with decreasing $\bar{M}_v$ and decreasing T_g[11], which are both lower for i-PMMA than for s-PMMA. The differing behaviour of PVF_2 in blends with i-PMMA, s-PMMA and a-PMMA appears to be related more to T_g than $\bar{M}_v$ since blends with a-PMMA show intermediate behaviour, while a-PMMA has the lowest value of $\bar{M}_v$. In view of the lower melt viscosity of i-PMMA in comparison with s-PMMA, one should expect a higher crystallization rate of PVF_2 in blends with i-PMMA. This may explain why PVF_2 starts to crystallize from blends with i-PMMA at a lower PVF_2 content than from blends with s-PMMA. This is corroborated by the higher crystallization temperatures T_c found in mixtures with i-PMMA during repeated scanning as shown in *Figure 5*. The same influence of melt viscosity on the crystallization rate of PVF_2 in PMMA containing blends, was also clearly demonstrated by Wang and Nishi[12].

An alternative explanation of the two T_g values in quenched PVF_2-rich samples could be found in liquid–liquid phase separation, followed by crystallization of PVF_2 in the PVF_2-rich phase. The phase diagram of PVF_2 with the PMMA's could show an upper critical solution temperature as proposed for the PVF_2/poly(ethyl methacrylate) system[13], or a lower critical solution temperature as theoretically predicted and observed by several authors[14-16]. In the case of liquid–liquid phase separation, PVF_2 has to crystallize in the PVF_2-rich phase either during quenching or later when the quenched sample is scanned in the d.s.c. The latter process can only be observed for PMMA contents in the range of 20–50 wt% and the crystallization temperature should be independent of the overall composition, since the separated phases have constant composition. However, the crystallization temperature of quenched PVF_2/a-PMMA samples shows a tremendous dependence on the composition (*Figure 7*), so we conclude that liquid–liquid phase separation of these polymers is very unlikely.

By means of curve fitting the single T_g values in *Figures 2, 3* and *4* can be adapted to the Gordon–Taylor relation[17], originally derived for copolymers:

$$T_g = \frac{c_2 T_{g_2} + c_1 k T_{g_1}}{c_2 + c_1 k}$$

In this study subscript 1 indicates the polymer with the higher T_g (PMMA) and 2 the polymer with the lower T_g (PVF_2), c = weight fraction, $k = \Delta_1 e / \Delta_2 e$ =

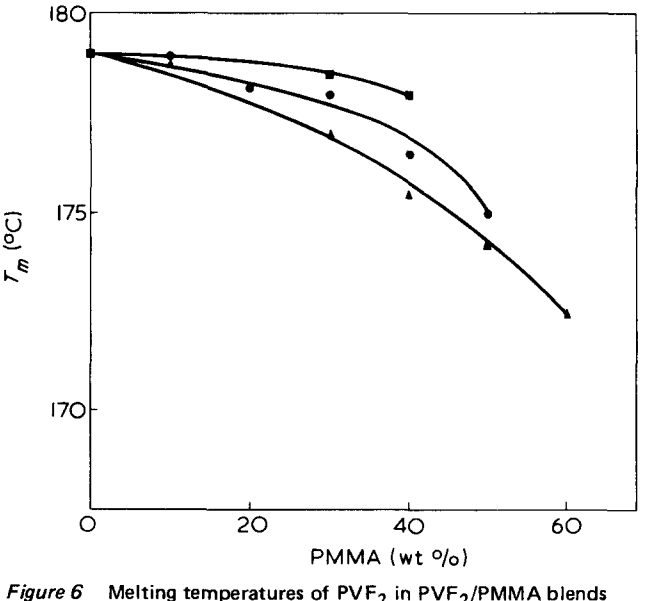

Figure 6 Melting temperatures of PVF_2 in PVF_2/PMMA blends isothermally crystallized at 155°C. ▲, PVF_2/i-PMMA; ●, PVF_2/a-PMMA; ■, PVF_2/s-PMMA

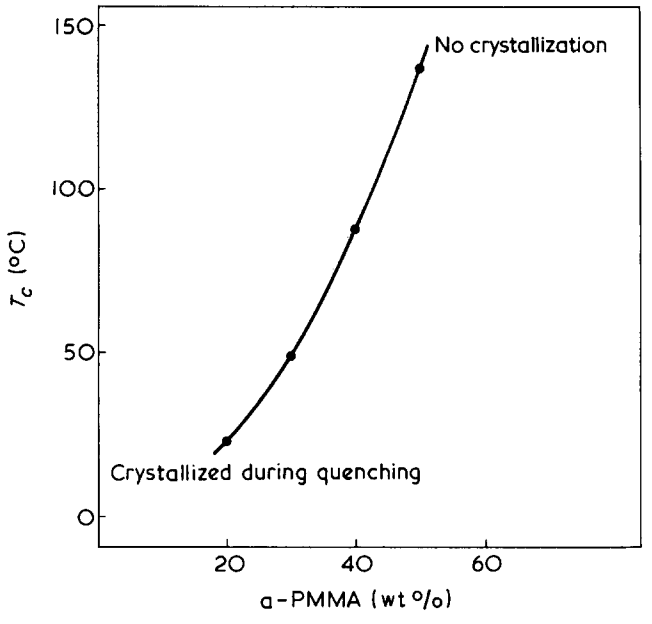

Figure 7 Crystallization temperatures of PVF_2 in blends with a-PMMA recorded with d.s.c. at a heating rate of 10°C/min, after quenching from the melt in liquid nitrogen

$(e_1 - e_g)_1/(e_1 - e_g)_2$, $e_{1,g} = (\partial v/\partial T)_p$, the thermal specific expansivity in the liquid and the glassy state, respectively (dim. cm^3/g K).

In *Figure 8* the solid curves represent the Gordon–Taylor relation with $k = 2.38$ for PVF_2/i-PMMA, $k = 1.72$ for PVF_2/a-PMMA and $k = 1.39$ for PVF_2/s-PMMA. Clearly, the experimental data are described quite well by these theoretical curves. From the adapted k values in the Gordon–Taylor relation for i-, a-, and s-PMMA, it can be concluded that Δe, the jump in thermal specific expansivity around T_g, has the highest value for i-PMMA and the lowest for s-PMMA. The observed difference in Δe of i- and s- PMMA confirms the results of other investigators[18] and can be explained by assuming that the α-transition (the main chain rotation) of the isotactic chains coincides with the general β-transition (the ester group rotation) of PMMA as has been previously suggested by Heyboer[19]. He found by dynamic–mechanical measurements the β-transition of 25°C, which is sufficiently apart from T_g of s-PMMA (130°C) but rather close to T_g of i-PMMA (51°C).

From literature[18] we know that $\Delta e = 4.3 \times 10^{-4}$ for i-PMMA and $\Delta e = 3.3 \times 10^{-4}$ for a-PMMA. With our k values of 2.38 and 1.72 for PVF_2/i-PMMA and PVF_2/a-PMMA, respectively, we could calculate then for PVF_2: $\Delta e = 1.9 \pm 0.1 \times 10^{-4}$. Finally, this result enabled us to calculate from our value $k = 1.39$ for PVF_2/s-PMMA a more reliable value $\Delta e = 2.6 \pm 0.1 \times 10^{-4}$ for s-PMMA. (s-PMMA in literature[18] showed too low a value of T_g.)

Melting point depressions in the blends

From the single glass transitions of quenched samples, it has already been concluded that PFV_2 is compatible with each of the three kinds of PMMA. Other indications for compatibility in the melt phase are the depressions of the melting point of PVF_2 by PMMA observed during repeated scanning (*Figure 5*) and isothermal crystallization (*Figure 6*), as well as the lowering of the crystallization temperature during repeated scanning (*Figure 5*).

As for low molecular weight solvents, the melting point depression exhibits a quantitative measure for the binary interaction parameter. For a mixture of two polymers Nishi and Wang[3] derived a relation between the melting point depression and the interaction parameter based upon Scott's thermodynamic theory for a mixture of two polymers[20]:

$$\frac{1}{T_m} = -\frac{R\ V_{2u}}{\Delta H_{fu}\ V_{1u}}\ \chi_{12}\ v_1^2 + \frac{1}{T_m^0} \qquad (1)$$

where V_{1u} = molar volume of the repeating units in PMMA (82.0, 83.3, and 84.0 cm^3/mol for i-, a-, and s-PMMA, respectively)[21]; V_{2u} = molar volume of the repeating units in PVF_2 = 35.6 cm^3/mol [21]; R = universal gas constant = 1.99 cal/mol K; ΔH_{fu} = molar heat of fusion of the repeating units in PVF_2 = 1.60 kcal/mol [22]; T_m = melting point of PVF_2 crystals in the mixture; T_m^0 = melting point in pure PVF_2; χ_{12} = binary interaction parameter; v_1 = volume fraction PMMA.

The binary interaction parameter is temperature dependent:

$$\chi_{12} = \frac{B\ V_{1u}}{RT} \qquad (2)$$

Substitution in equation (1) results in:

$$\frac{1}{T_m} = -\frac{V_{2u} B v_1^2}{\Delta H_{fu}\ T_m} + \frac{1}{T_m^0} \qquad (3)$$

The interaction energy density B can thus be calculated from the slope of the plot $1/T_m$ as a function of v_1^2/T_m. Equation (3) is entirely based on thermodynamics and does not take into account morphological effects such as size and perfection of the crystals, which can give rise to large deviations in the melting points of polymers[23].

So, one should finally prefer to study the influence of different tacticities of PMMA on the interaction of PVF_2 under mutually comparable crystallization conditions.

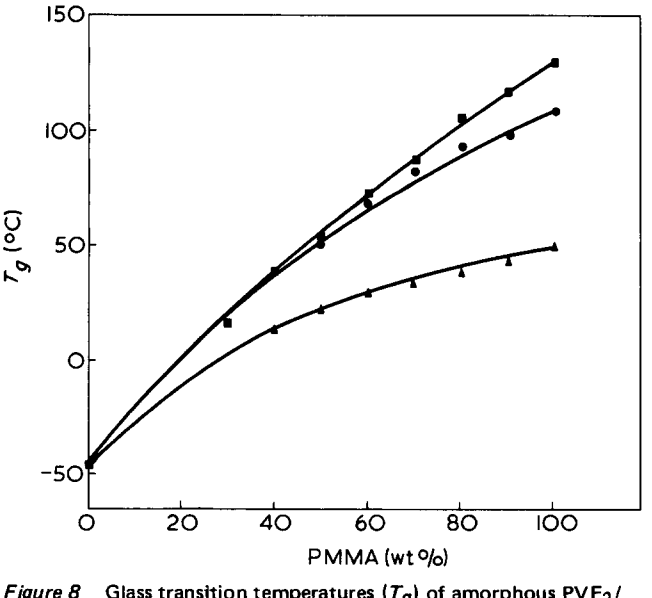

Figure 8 Glass transition temperatures (T_g) of amorphous PVF_2/PMMA blends after quenching from the melt in liquid nitrogen. ▲, PVF_2/i-PMMA; ●, PVF_2/a-PMMA; ■, PVF_2/s-PMMA. ——, are calculated with the theoretical Gordon–Taylor relation

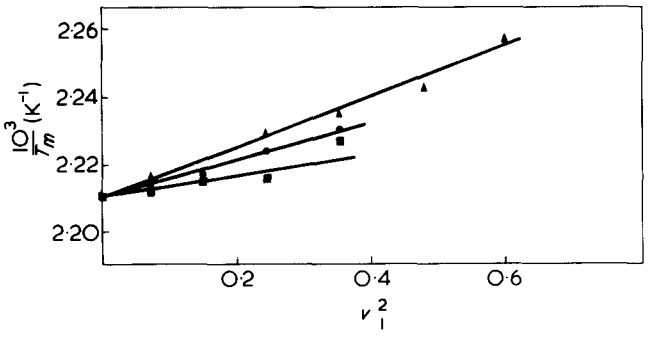

Figure 9 Depression of melting point T_m of PVF_2 in PVF_2/i-PMMA blends (▲), PVF_2/a-PMMA blends (●) and PVF_2/s-PMMA blends (■), crystallized at a constant temperature of 155°C (plotted according to equation (1); v_1 = volume fraction i-, a-, or s-PMMA).

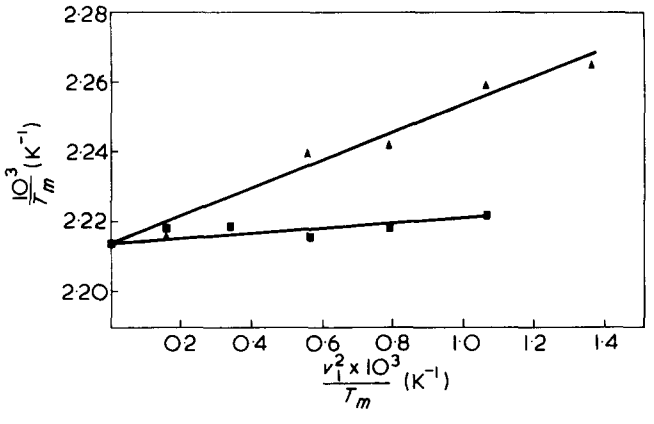

Figure 10 Depression of melting point T_m of PVF_2 in PVF_2/i-PMMA blends (▲) and PVF_2/s-PMMA blends (■), crystallized at a constant relative undercooling of 0.07, (plotted according to equation (3); v_1 = volume fraction i- or s-PMMA)

Table 2 Interaction parameters derived from melting point depressions at constant relative undercoolings

Relative undercooling, $(T_m^* - T_c)/T_m^*$	Interaction energy density B (cal/cm^3)		Difference in interaction, ΔB
	i-PMMA/PVF_2	s-PMMA/PVF_2	
0.10	−2.20	−1.21	1.0
0.09	−2.07	−0.90	1.2
0.08	−1.80	−0.54	1.3
0.07	−1.71	−0.27	1.4
0.06	−1.26	0	1.3

The results of the repeated scanning procedure (*Figure 5*) produce a first indication of a stronger interaction of PVF_2 with i-PMMA. In spite of the higher crystallization temperatures, resulting in more perfect crystals, the melting temperatures of PVF_2 are lower in the i-PMMA containing blends than in those with a- and s-PMMA. According to equation (1) this means that the binary interaction parameter χ_{12} is lowest for i-PMMA/PVF_2. However, because of the kinetic effects on polymer crystallization during cooling, large differences in crystallization temperatures are found for the three blends *(Figure 5)*.

PVF_2 needs a larger undercooling for crystallization in our s-PMMA containing blends than in i-PMMA and a-PMMA containing blends. due to the higher melt viscosity, as discussed before. Therefore, it is clear that the results of such dynamic crystallization experiments are unsuitable for a quantitative analysis of melting point depressions.

A first improvement was obtained by applying constant crystallization temperatures. The results of such isothermal crystallization also indicate a stronger interaction of i-PMMA with PVF_2, since all crystallization temperatures between 95° and 165°C produce the largest melting point depressions in the i-PMMA containing blends. The results of isothermal crystallization at 155°C are shown in *Figure 6* and clearly demonstrate that the absence of kinetic effects drastically diminishes the melting point depression. Because of the rather low crystallization temperature the undercoolings did not differ strongly, which permitted us to evaluate the data from *Figure 6* in terms of equation (1). The result is shown in *Figure 9* and leads to the following values of χ_{12} at melting temperatures around 177°C: $\chi_{12} = -0.13$ for i-PMMA/PVF_2; $\chi_{12} = -0.10$ for a-PMMA/PVF_2; $\chi_{12} = -0.06$ for s-PMMA/PVF_2.

For a better estimation of the differences in interaction parameter of i- and s-PMMA with PVF_2, we tried to reduce even more the influence of the crystal morphology on the melting points by choosing small and constant relative undercoolings $(T_m^* - T_c)/T_m^*$ for these blends. Here T_m^* is the equilibrium melting point of PVF_2 crystals in a blend as found by extrapolation in a $T_m - T_c$ diagram according to Hoffman and Weeks[23]. For undiluted PVF_2 we found $T_m^* = 183.8° \pm 0.5$°C, in good agreement with literature values[24,25]. In our study all PVF_2 crystals were in the low-melting form II, as has been confirmed by X-ray diffraction[26].

In *Figure 10* we plotted $1/T_m$ vs. v_1^2/T_m according to equation (3) for a constant and small relative undercooling of 0.07. A least squares fit resulted in slopes of 0.038 and 0.006, corresponding to B values of −1.71 and −0.27 cal/cm^3, for i-PMMA/PVF_2 and s-PMMA/PVF_2 respectively. *Table 2* shows that the interaction of PVF_2 with i-PMMA is stronger than with s-PMMA, irrespective of the relative undercooling. Although both B values are decreasing with increasing relative undercooling, their difference ΔB remains fairly constant.

From this temperature dependence it is clear that these B values obtained for constant relative undercooling include still some contributions of morphological effects. However, the constant difference ΔB between s-PMMA/PVF_2 and i-PMMA/PVF_2 should represent the difference in thermodynamic interaction. Substitution of B into equation (2) yields the following χ_{12} values for $T = 175$°C: $\chi_{12} = -0.1$ for i-PMMA/PVF_2; $\chi_{12} = 0$ for s-PMMA/PVF_2.

The difference with the values obtained from isothermal crystallization experiments is clear and has to be attributed to larger contributions of non-thermodynamic effects in these experiments.

REFERENCES

1 Noland, J. S., Hsu, N. N. C., Saxon, R. and Schmitt, J. M. *Adv. Chem. Ser.* 1971, **99**, 15
2 Paul, D. R. and Altamirano, J. O. *Polym. Prepr.* 1974, **15**, 409
3 Nishi, T. and Wang, T. T. *Macromolecules* 1975, **8**, 909
4 Schurer, J. W., de Boer, A. and Challa, G. *Polymer* 1975, **16**, 201
5 Goode, W. E., Owens, F. H., Feldmann, R. P., Snijder, W. H. and Moore, J. H. *J. Polym. Sci.* 1960, **46**, 317
6 Abe, H., Imai, K. and Matsumoto, M. *J. Polym. Sci. (C)* 1968, **23**, 469
7 Ramey, K. C. *J. Polym. Sci. (B)* 1967, **5**, 859

8 Bischof, J. and Desreux, V. *Bull. Soc. Chim. Belg.* 1952, **61**, 10
9 Richardson, M. J. and Saville, N. G. *Polymer* 1975, **16**, 753
10 Boyer, R. F. *J. Macromol. Sci. (B)* 1973, **8**, 503
11 Williams, M. L., Landel, R. F. and Ferry, J. D. *J. Am. Chem. Soc.* 1955, **77**, 3701
12 Wang, T. T. and Nishi, T. *Macromolecules* 1977, **10**, 421
13 Kwei, T. K., Patterson, G. W. and Wang, T. T. *Macromolecules* 1976, **9**, 780
14 McMaster, A. P. *Macromolecules* 1973, **6**, 760
15 Orwoll, R. A. and Flory, P. J. *J. Am. Chem. Soc.* 1967, **89**, 6814
16 Höcker, H., Shih, H. and Flory, P. J. *Trans. Faraday Soc.* 1971, **67**, 2275.
17 Gordon, M. and Taylor, J. S. *J. Appl. Chem.* 1952, **2**, 493
18 Bywater, S. and Toporowski, P. M. *Polymer* 1972, **13**, 94
19 Heyboer, J. in 'Physics of Non-crystalline Solids', (Ed. J. A. Prins), North Holland, Amsterdam, 1965, p 231
20 Scott, R. L. *J. Chem. Phys.* 1949, **17**, 279
21 Joshi, R. M. in 'Encyclopedia of Polymer Science and Technology', (Eds F. H. Mark and G. N. Gaylord), Interscience, New York, 1970, Vol. 13, p 788
22 Nakagawa, K. and Ishida, Y. *J. Polym. Sci. (Polym. Phys. Edn)* 1973, **11**, 2153
23 Hoffman, J. D. and Weeks, J. J. *J. Res. Nat. Bur. Stand. (A)* 1962, **66**, 13
24 Welch, G. J. and Miller, R. L. *J. Polym. Sci. (Polym. Phys. Edn)* 1976, **14**, 1683
25 Osaki, S. and Ishida, Y. *J. Polym. Sci. (Polym. Phys. Edn)* 1975, **12**, 1071
26 Hasegawa, R., Takahashi, Y., Chatani, Y. and Tadokoro, H. *Polym. J.* 1972, **3**, 600